Constructing Dependence of Electrical Parameters on Porosity and Water Saturation for Digital Models of High-Permeability Rock Samples

Tatyana Khachkova[1(✉)], Vadim Lisitsa[2], Vladislav Krutko[3], and Alexander Avdonin[3]

[1] Institute of Petroleum Geology and Geophysics SB RAS, Koptug ave. 3, Novosibirsk 630090, Russia
KhachkovaTS@ipgg.sbras.ru
[2] Institute of Mathematics SB RAS, Koptug ave. 2, Novosibirsk 630090, Russia
[3] Gazpromneft NTC, Moika River emb. 75-79 D, Saint-Petersburg 190000, Russia

Abstract. The present study focuses on the numerical evaluation of Archie's coefficients – specifically, the cementation parameter and saturation exponent – using a digital model of a high-permeability rock sample. Accurate estimation of these parameters is critical for reservoir development planning and optimizing hydrocarbon recovery through formation stimulation techniques.

To derive the coefficients, we construct two relationships: the formation factor versus porosity and the resistivity index versus water saturation. The paper presents a methodology and case studies for establishing these dependencies. The proposed approach involves solving two optimization problems to perform a linear regression in a logarithmic scale, based on both the generalized and classical forms of Archie's law.

Keywords: Electrical parameters · Formation factor · Porosity · Resistivity index · Water saturation · Digital models · High-permeability samples · CT-images

1 Introduction

In recent years, there has been a rapid development of numerical methods for rock characterization. The achievements are driven by three key factors: (1) improvements in X-ray tomography resolution, enabling the generation of highly accurate three-dimensional rock models; (2) increased computational power of modern systems; and (3) progress in numerical algorithms, which together facilitate pore-scale simulation of complex physical and chemical processes.

To date, numerous algorithms have been developed to estimate key petrophysical parameters, including porosity, absolute permeability [2,7,12,13], relative permeabilities [1,3,11], elastic moduli [2,9,14,16], electrical resistivity [2,10,18], geometric and topological pore-space characteristics [5], etc. These computational tools enable researchers to investigate relationships between rock

© The Author(s), under exclusive license to Springer Nature Switzerland AG 2026
O. Gervasi et al. (Eds.): ICCSA 2025 Workshops, LNCS 15888, pp. 419–432, 2026.
https://doi.org/10.1007/978-3-031-97596-7_28

properties, analyze an influence of various factors on estimates, predict a behavior of the objects under study and so on.

The present work focuses on the electrical properties of reservoir rocks. As hydrocarbon reserves are typically quantified using electrical logging data – interpreted through Archie's empirical laws – accurate determination of Archie's coefficients (the cementation parameter m and saturation exponent n) is critical for reservoir development and enhanced hydrocarbon recovery strategies. However, the conventional Archie's model (m = 2, n = 2) applies only to clean, water-wet rocks, a condition rarely met in natural reservoirs [15].

To extend Archie's framework to other rocks, it's constructed two key relationships: (1) the formation factor versus porosity and (2) the resistivity index versus water saturation. We propose a methodology for deriving these dependencies using digital rock models of high-permeability samples, combining numerical simulations with optimization-based regression analysis.

For a monomineralic rock saturated with a single-phase formation fluid, the formation factor (F) is defined as the ratio of the rock's electrical resistivity ($\hat{\rho}$) to the fluid's electrical resistivity (ρ^{fl}):

$$F = \frac{\hat{\rho}}{\rho^{fl}}.$$

This definition is applied when the resistivity of the rock's mineral matrix ρ^s is significantly higher than that of the fluid. Thus, typical resistivity values for mineralized fluids are below unity ($\rho^{fl} < 1$), while dielectric minerals (quartz, micas, feldspars, etc.) exhibit extremely high resistivities ($\rho^s = 10^{12} - 10^{15}$). Semiconductor minerals (carbonates, sulfates, halides, etc.) also demonstrate relatively high resistivity ($\rho^s = 10^4 - 10^8$). In contrast, clay minerals (hydromicas, montmorillomonite, kaolinite, etc.) are characterized by substantially lower resistivities ($\rho \leq 10^4$). Consequently, for rocks composed primarily of minerals from the first two categories, the formation factor can serve as a quantitative characteristic of the pore space structure, since a rock conductivity is provided exclusively by the fluid phase. However, the contribution of clay minerals cannot be neglected, in which case the formation factor no longer represents pore space characteristics alone.

In this study, it is assumed that only dielectric or semiconductor rocks are considered. In this case, it follows from physical considerations that with a porosity equal to one, the entire volume under study will be occupied by fluid, and the resistivity of the entire "sample" will exactly coincide with that of the fluid. In this case, the formation factor will be equal to one. If there are no pores in the sample, or only isolated pores are present, the formation factor is close to zero. Based on experimental data, Archie's empirical law [4] was established, which relates the formation factor to the rock porosity (φ) through the equation:

$$F(\varphi) = \varphi^{-m}, \tag{1}$$

where m is the cementation parameter characterizing a specific rock. Later, in the work [17], a correction of this equation was proposed:

$$F(\varphi) = \alpha\varphi^{-m}, \tag{2}$$

where parameter α is the tortuosity of the pore space. Both parameters are empirically derived as regression coefficients.

Archie's laws also establish relationships between other key parameters: the resistivity index (RI) and water saturation (S_w). Recall that the resistivity index represents the ratio between the rock (formation) electrical resistivity ρ_t at partial water saturation S_w and the resistivity ρ_0 of the fully water-saturated rock (formation):

$$RI = \frac{\rho_t}{\rho_0}.$$

The classical form of Archie's law for the resistivity index is expressed as:

$$RI(S_w) = S_w^{-n}, \tag{3}$$

where n is the saturation exponent. The generalized Archie's law can be written as:

$$RI(S_w) = \alpha S_w^{-n}, \tag{4}$$

where parameter α is the saturation distribution factor.

The following section details the mathematical framework for constructing such dependencies, using the formation factor and porosity as an example.

2 Theoretical Foundations of Constructing Dependencies

Let the formation factors $F_1, ..., F_N$ be known for a set of N samples with porosity values $\varphi_1, ..., \varphi_N$, then the formula (2) can be conveniently written as:

$$\ln F = \ln \alpha - m \ln \varphi,$$

that is, on a logarithmic scale, Archie's law describes a linear relationship between the logarithms of the formation factor and the porosity. If we assume that the results of numerical simulations must satisfy the formula specified, then for all $j = 1, ..., N$ the following relationships must be satisfied:

$$\ln F_j = \ln \alpha - m \ln \varphi_j,$$

as a result, an overdetermined system of linear equations was obtained for determining the parameters $\ln \alpha$ and m:

$$\begin{pmatrix} 1 & -\ln \varphi_1 \\ 1 & -\ln \varphi_2 \\ \vdots & \vdots \\ 1 & -\ln \varphi_N \end{pmatrix} \begin{pmatrix} \ln \alpha \\ m \end{pmatrix} = \begin{pmatrix} \ln F_1 \\ \ln F_2 \\ \vdots \\ \ln F_N \end{pmatrix}.$$

The solution of such a system can be obtained in a generalized sense [8], that is, one that minimizes the discrepancy. To construct this solution, it is sufficient to consider the problem:

$$\begin{pmatrix} 1 & \dots & 1 \\ -\ln\varphi_1 & \dots & -\ln\varphi_N \end{pmatrix} \begin{pmatrix} 1 & -\ln\varphi_1 \\ 1 & -\ln\varphi_2 \\ \vdots & \vdots \\ 1 & -\ln\varphi_N \end{pmatrix} \begin{pmatrix} \ln\alpha \\ m \end{pmatrix} = \begin{pmatrix} 1 & \dots & 1 \\ -\ln\varphi_1 & \dots & -\ln\varphi_N \end{pmatrix} \begin{pmatrix} \ln F_1 \\ \ln F_2 \\ \vdots \\ \ln F_N \end{pmatrix}$$

or

$$\begin{pmatrix} N & -\sum \ln\varphi_j \\ -\sum \ln\varphi_j & \sum(\ln\varphi_j)^2 \end{pmatrix} \begin{pmatrix} \ln\alpha \\ m \end{pmatrix} = \begin{pmatrix} \sum \ln F_j \\ -\sum \ln\varphi_j \ln F_j \end{pmatrix}.$$

The resulting system is easily solvable, and its solution exactly coincides with the generalized solution of the original system of equations. Although its condition number can be quite high if the range of porosity variation is small.

This solution minimizes the discrepancy:

$$r = \sqrt{\sum_{j=1}^{N} (\ln F_j - \ln\alpha + m\ln\varphi_j)^2}.$$

It should be understood that this solution is not a solution to the minimization problem

$$\sum_{j=1}^{N} (F_j - \alpha\varphi_j^{-m})^2 \to \min,$$

however, if we represent the residual vector $\boldsymbol{r}$ in the form

$$r_j = \ln F_j - \ln\alpha + m\ln\varphi_j,$$

assuming that $r_j << 1$ (otherwise it is possible to perform normalization by considering, for example, $r_j/\|\ln F\|$), then the following representation is true:

$$\frac{F_j}{\alpha\varphi_j^m} - 1 = e^{r_j} - 1.$$

Respectively,

$$\sum_{j=1}^{N} \left(\frac{F_j}{\alpha\varphi_j^m} - 1\right)^2 = \sum_{j=1}^{N} (e^{r_j} - 1)^2 = \sum_{j=1}^{N} r_j^2 + O(|r|^3).$$

That is, assuming the residual is small on a logarithmic scale, the resulting solution will be a fairly accurate approximation of the solution to the minimization problem.

$$\sum_{j=1}^{N} \left(\frac{F_j}{\alpha\varphi_j^m} - 1\right)^2 \to \min.$$

If it is necessary to refine the obtained solution, gradient methods can be used.

Further analysis of the quality of the obtained solution will be carried out on a logarithmic scale. It is convenient to introduce two measures. The first is the relative norm of the discrepancy:

$$R = \frac{r}{\| \ln F_j \|_2} = \frac{\sqrt{\sum_{j=1}^{N} (\ln F_j - \ln \alpha + m \ln \varphi_j)^2}}{\sqrt{\sum_{j=1}^{N} (\ln F_j)^2}},$$

the second is the reliability coefficient, defined as

$$R^2 = 1 - \frac{r^2}{\sigma(F_j)} = 1 - \frac{\sum_{j=1}^{N} (\ln F_j - \ln \alpha + m \ln \varphi_j)^2}{\sum_{j=1}^{N} (\ln F_j - < \ln F_j >)^2},$$

where $<>$ - denotes the average value. That is, R^2 determines the proximity of the residual to the standard deviation of the measurements.

The minimization algorithm described above allows constructing the dependence of the formation factor on porosity according to the modified Archie law, which takes into account the tortuosity parameter α. If Archie's law is considered in the classical formulation, that is, with $\alpha = 1$, then the minimization problem is written as:

$$\sum_{j=1}^{N} (\ln F_j + m \ln \varphi_j)^2 \to \min,$$

or in the form of a problem of finding a generalized solution to a system of linear algebraic equations of the form:

$$\begin{pmatrix} -\ln \varphi_1 \\ -\ln \varphi_2 \\ \vdots \\ -\ln \varphi_N \end{pmatrix} (m) = \begin{pmatrix} \ln F_1 \\ \ln F_2 \\ \vdots \\ \ln F_N \end{pmatrix}$$

or

$$\sum_{j=1}^{N} (\ln \varphi)^2 \, m = \sum_{j=1}^{N} \ln F_j \ln \varphi_j.$$

Obviously, all the above considerations about the accuracy assessment and the reliability coefficient remain true in the simplified case under consideration. However, due to the fact that optimization is carried out relative to only one parameter, the error value is expected to be higher.

3 Constructing the Dependence of the Formation Factor on the Porosity for Digital Models

3.1 Digital Models of High-Permeability Rock Samples

In this part of study, we consider two digital models of high-permeability sandstone:

1. Berea sandstone model with 'VSG reference segmentation' from the benchmarks study [2].
2. Bentheimer sandstone model obtained from the DigitalRocksPortal repository (project ID 317: '11 Sandstones: raw, filtered and segmented data').

Two-dimensional cross-sections of both samples are presented in the Fig. 1. The Berea sandstone model has dimensions of $724 \times 724 \times 1024$ voxels at 0.74 um/voxel resolution, with a porosity of 18.4%. The Bentheimer model size is $1000 \times 1000 \times 1000$ voxels at 2.25 um/voxel resolution, and a porosity is 26.7%.

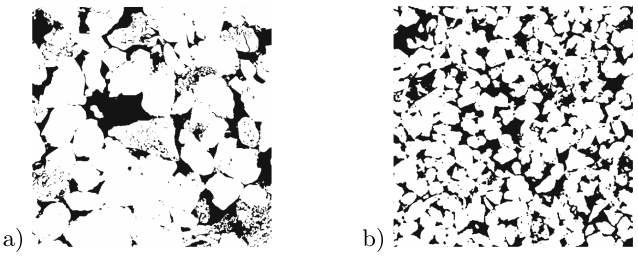

Fig. 1. Two-dimensional cross-sections of high-permeability sandstone models: a) Berea (0.74 um); b) Bentheimer (2.25 um).

To validate our computational results, we employ the digital rock physics benchmarks from [2]. This reference presents calculated by different methods formation factors for digital Berea sandstone samples with varying segmentation approaches and porosity values, as shown in their Fig. 7b. For verification purposes, we reproduce this figure (including legend) below as Fig. 2.

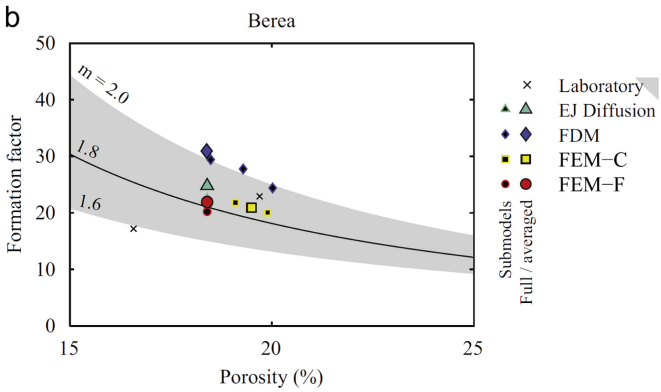

Fig. 2. Figure 7b from [2]. The values of formation factor calculated for a Berea sandstone samples. The gray shaded area and solid line represent Archie's law with different cementation factors.

3.2 Numerical Experiments

To construct the dependence of the formation factor on the porosity of the digital models, each model was divided into cubic subsamples of 400^3 voxels. The 1000^3 Bentheimer sample was partitioned into 3 segments along each axis (resulting in 27 subsamples), while the smaller Berea sample was divided into 2 segments along the X and Y axes and 3 segments along the Z axis (yielding 12 subsamples).

For each full-size digital sample and all subsamples, the porosity values were calculated first, followed by the resistivity and formation factor values for each of the three directions (calculating the values of the electrical resistivity and resistivity index were carried out using a solver belonging to Gazpromneft NTC). After that, the mean values were obtained by arithmetic averaging across the three spatial directions. The calculated formation factor values for all digital samples are presented in Figs. 3 - 4. In addition to the values obtained, the plots include curves representing Archie's law for the formation factor and the porosity: $F = \varphi^{-m}$. For the cementation parameter m, the values of 1.6, 1.8, 2.0 were used from [2].

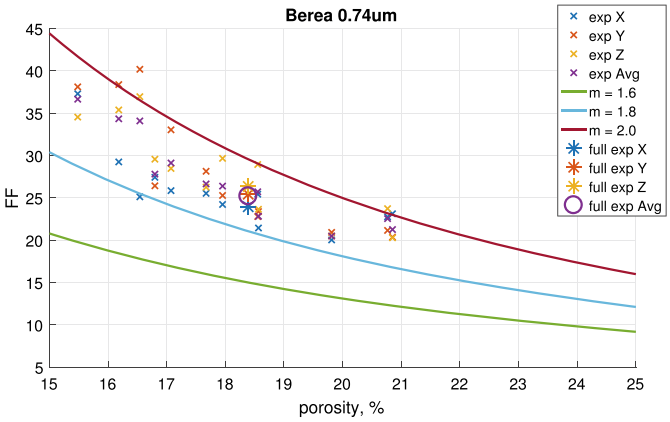

Fig. 3. Calculated formation factor values for the full-size Berea (0.74 um) digital sample and all its 400^3-voxel subsamples.

A comparison of our calculation results for the full-size samples (Fig. 3) with the benchmarks from [2] (Fig. 2) reveals excellent agreement between the values. The closest match is observed with the results obtained by the EJ Diffusion method in the cited study. Furthermore, Fig. 3 demonstrates that both the formation factor of the full-size sample and its subsamples fall well within the range of cementation parameters ($m \in [1.6, 2.0]$) proposed by [2]. This consistency is also evident for the Bentheimer sample (Fig. 4), where all calculated values align perfectly with the same range of cementation parameters.

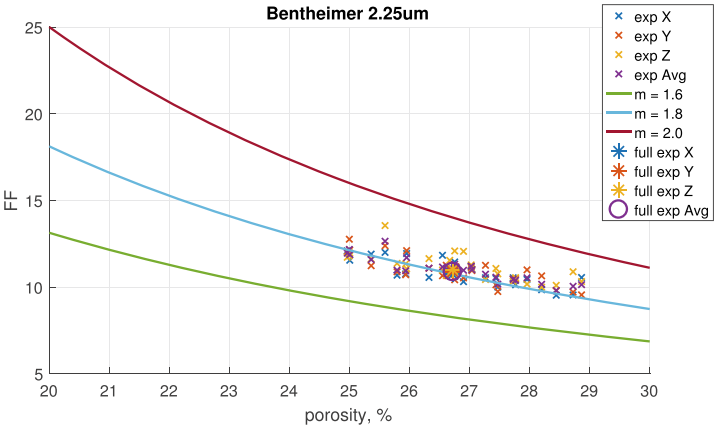

Fig. 4. Calculated formation factor values for full-size Bentheimer (2.25 um) digital sample and all its 400^3-voxel subsamples.

Next, to construct the dependencies of the formation factor on porosity, the methodology outlined in Sect. 2 was applied to our numerical results. Figures 5 and 6 present the numerical experiment results for all rock subsamples, along with estimated formation factor – porosity dependencies obtained by solving two optimization problems. The solid curves represent fits based on the generalized Archie's law, while the dashed curves correspond to the classical Archie's law formulation (where $\alpha = 1$). Tables 1 and 2 provide the calculated values of the parameters α and m, along with the relative residual and the parameter R^2 values for each sample and for two different approximations.

Table 1. Approximation of the dependence of the formation factor on porosity for the Berea (0.74 um) digital model.

	$F = \alpha\varphi^{-m}$				$\tilde{F} = \varphi^{-m}$		
	α	m	res	R^2	m	res	R^2
X	2.58	1.33	0.028	0.64	1.88	0.032	0.53
Y	0.46	2.38	0.03	0.82	1.92	0.033	0.79
Z	1.15	2.85	0.026	0.79	1.93	0.026	0.79
All	1.1	1.85	0.033	0.71	1.91	0.033	0.71

The tables reveal that, when applying the generalized Archie's law, there is a stable difference in the regression coefficient estimates depending on the direction in which the resistivity assessment was carried out. A possible reason for such a discrepancy may be attributed to the anisotropic geometry and topological complexity of the pore space. In contrast, when applying the Archie's law in the

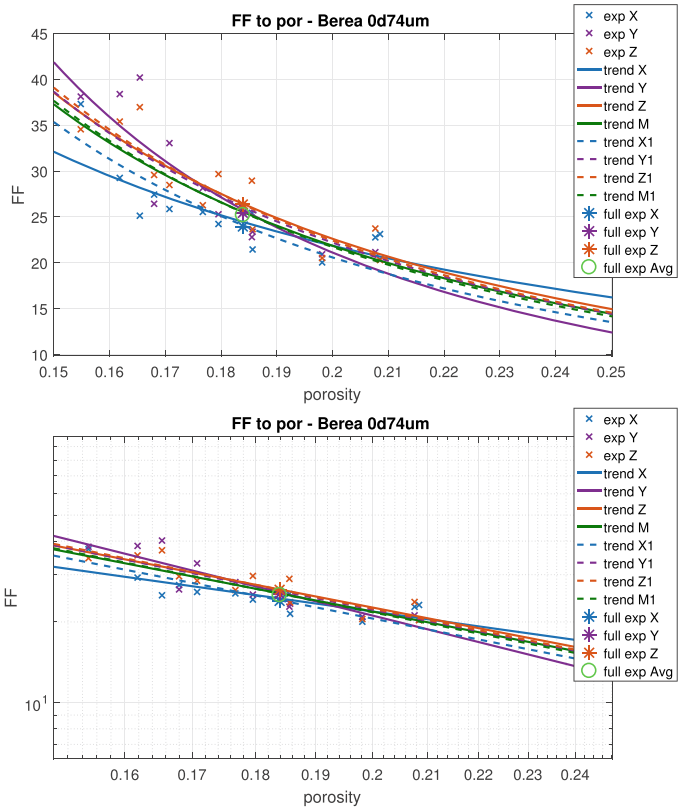

Fig. 5. The dependence of the formation factor on porosity for Berea (0.74 um) sandstone in linear and logarithmic scale.

Table 2. Approximation of the dependence of the formation factor on porosity for the Bentheimer (2.25 um) digital model.

	$F = \alpha\varphi^{-m}$				$\tilde{F} = \varphi^{-m}$		
	α	m	res	R^2	m	res	R^2
X	1.8	1.37	0.017	0.67	1.81	0.018	0.6
Y	1.58	1.47	0.018	0.86	1.81	0.019	0.64
Z	2.36	1.18	0.019	0.53	1.83	0.022	0.37
All	1.88	1.34	0.018	0.61	1.82	0.02	0.53

classical formulation, the estimates of the cementation parameter coefficients are close to each other. In addition, they are in very good agreement with the source [2]. However, applying the generalized Archie's law often demonstrates a significant deviations of the coefficient α from unity, as well as a reduced relative

residuals and higher values of the coefficient R^2. Consequently, the usage of such form allows to significantly increase the accuracy of the approximation.

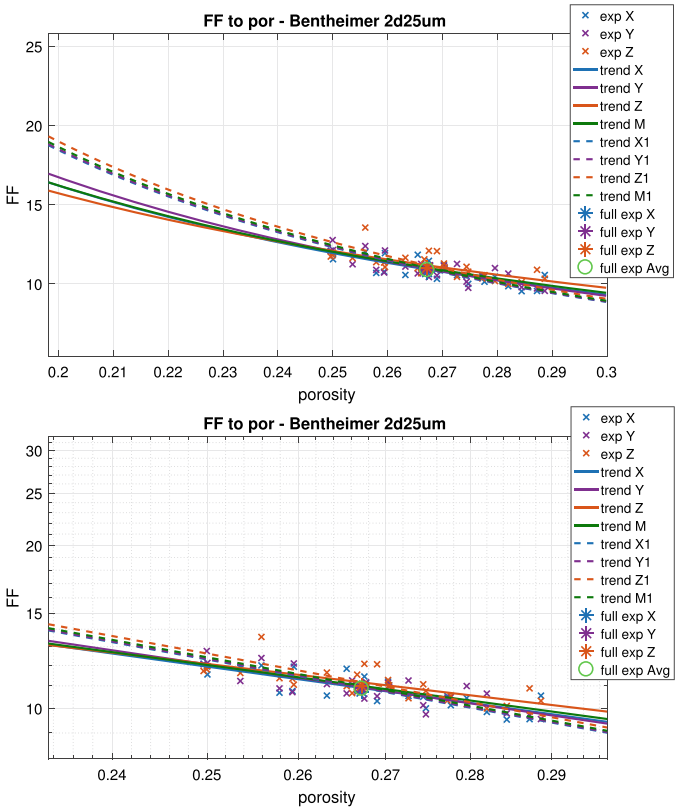

Fig. 6. The dependence of the formation factor on porosity for Bentheimer (2.25 um) sandstone in linear and logarithmic scales.

4 Constructing the Dependence of the Resistivity Index on the Water Saturation for Digital Models

In this part of work, we considered Berea sandstone model obtained from the DigitalRocksPortal repository (project ID 317: '11 Sandstones: raw, filtered and segmented data'). The model size is $1000 \times 1000 \times 1000$ at 2.25 um/voxel resolution and the porosity is 21.7%.

The resistivity index – water saturation (RI – S_w) relationship is constructed using partially water-saturated rock models. These model sets are generated through either:

1. Primary drainage simulation, where the non-wetting phase displaces the wetting phase;
2. Imbibition simulation, where the wetting phase gradually displaces the non-wetting one, as that the wetting phase fraction in the pumped mixture progressively increasing during each imbibition cycle.

In this study, we first simulated primary drainage for the selected rock sample, generating a set of models with varying water saturations. For each model, we calculated both the water saturation and resistivity index.

Subsequently, we performed imbibition simulations using three irreducible water saturation values (S_{wir} = 0.05, 0.2, 0.3), conducting three parallel simulation scenarios. This produced distinct sets of partially saturated models for each S_{wir} case. Similar to the drainage case, we computed the key parameters (RI and S_w) for all models.

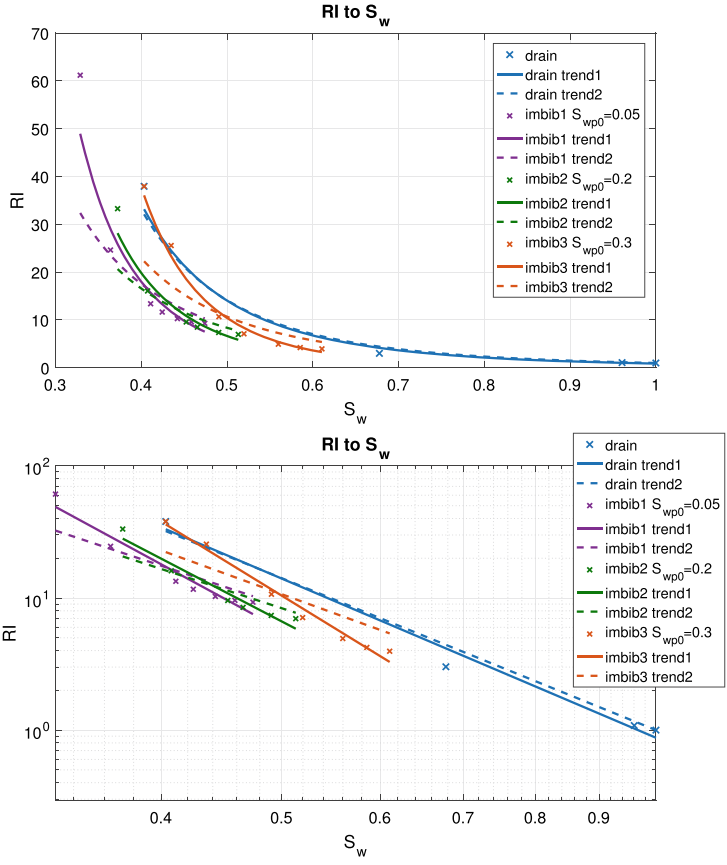

Fig. 7. The dependence of the resistivity index on water saturation for Berea (2.25 um) sandstone in linear and logarithmic scales.

Using these datasets, we solved two optimization problems to construct linear regressions. Figure 7 presents the saturation parameter versus water saturation relationships for both drainage and imbibition cases. The solid curves represent the trends derived from the generalized Archie's law, while the dashed curves correspond to the classical Archie's law formulation with $\alpha = 1$.

Table 3 summarizes the results: $RI - S_w$ dependencies obtained for drainage case and for three distinct imbibition scenarios. The table includes the coefficients α and n, along with the relative residual (res) and coefficient of determination (R^2) values for both approximation methods.

Table 3. Approximation of the dependence of the resistibity index on water saturation for the Berea (2.25 um) model.

	$RI = \alpha S_w^{-n}$				$\tilde{RI} = S_w^{-n}$		
	α	n	res	R^2	n	res	R^2
Drainage	0.88	4.00	0.098	0.98	3.82	0.112	0.98
Imbib, $S_{wir} = 0.05$	0.17	5.11	0.055	0.94	3.13	0.102	0.80
Imbib, $S_{wir} = 0.2$	0.22	4.90	0.052	0.94	3.07	0.096	0.81
Imbib, $S_{wir} = 0.3$	0.19	5.78	0.047	0.98	3.42	0.152	0.81

The results demonstrate that when applying the generalized Archie's law, the regression coefficients for imbibition vary significantly depending on the irreducible water saturation (S_{wir}). At the same time, using the classical Archie's law

TABLE 2—WETTABILITY vs. SATURATION EXPONENT AT 77°F FOR BEREA AND ELGIN SANDSTONES AND A SET OF DIFFERENT CRUDE OILS DESIGNATED BY API GRAVITY (after Siddiqui [14])

Core	I_w	n	γ_o (°API)
	Berea Cores		
101	0.463	2.71	39
102	0.430	1.54	42
103	0.430	2.76	38
104	0.392	2.18	41
105	0.358	2.95	38
106	0.231	3.90	36
107	0.187	3.35	35
108	0.185	3.58	32
109	0.181	3.62	37
110	0.169	3.43	32
111	0.127	4.00	37
112	0.101	3.17	35

Fig. 8. Table 2 from [6] presents laboratory experimental data for Berea sandstone samples.

formulation gives closer saturation exponent values across all imbibition cases. Furthermore, these classical Archie's law estimates show excellent agreement with laboratory measurements reported in [6]. Figure 8 reproduces Table 2 from [6], presenting experimental data for Berea sandstone samples. The measured saturation exponents range from 1.54 to 4.0, with a mean value of 3.1. Notably, our numerically derived saturation exponent for imbibition (3.2) closely matches this laboratory average.

5 Conclusion

The present study focuses on the numerical evaluation of Archie's coefficients – specifically, the cementation parameter and saturation exponent – using a digital model of a high-permeability rock sample. Accurate estimation of these parameters is critical for reservoir development planning and optimizing hydrocarbon recovery through formation stimulation techniques.

To derive the coefficients, we construct two relationships: the formation factor versus porosity and the resistivity index versus water saturation. The paper presents a methodology and case studies for establishing these dependencies. The proposed approach involves solving two optimization problems to perform a linear regression in a logarithmic scale, based on both the generalized and classical forms of Archie's law.

The presented results reveal a significant discrepancy in the regression coefficient estimates when applying the generalized Archie's law, dependent on (1) the direction of resistivity assessment (for $F-\varphi$ dependence); (2) the irreducible water saturation (for $RI - S_w$ dependence). In contrast, the classical form of Archie's law yields cementation parameter (saturation exponent) estimates that are mutually consistent across all direction (imbibition cases) and are in good agreement with the values reported by [2,6].

However, the generalized Archie's law frequently produces a coefficient α significantly deviating from 1, while exhibiting reduced relative residual and higher R^2 values. These results indicate that the generalized form substantially improves approximation accuracy compared to the classical model.

Acknowledgments. T. Khachkova performed numerical simulations under the support of Russian Science Foundation (grant no. 25-21-00352, https://rscf.ru/en/project/25-21-00352/)

References

1. Alpak, F.O., Riviere, B., Frank, F.: A phase-field method for the direct simulation of two-phase flows in pore-scale media using a non-equilibrium wetting boundary condition. Comput. Geosci. **20**(5), 881–908 (2016). https://doi.org/10.1007/s10596-015-9551-2
2. Andra, H., et al.: Digital rock physics benchmarks - Part II: computing effective properties. Comput. Geosci. **50**, 33–43 (2013)

3. Apourvari, S.N., Arns, C.H.: Image-based relative permeability upscaling from the pore scale. In: Advances in Water Resources (2015)
4. Archie, G.E.: Classification of carbonate reservoir rocks and petrophysical considerations. AAPG Bull. **36**(2), 278–298 (1952)
5. Bazaikin, Y.V., Malkovich, E.G., Derevschikov, V.S., Lysikov, A.I., Okunev, A.G.: Evolution of sorptive and textural properties of CaO-based sorbents during repetitive sorption/regeneration cycles. Chem. Eng. Sci. **152**, 709–716 (2016)
6. Donaldson, E.C., Siddiqui, T.K.: Relationship between the archie saturation exponent and wettability. SPE Form. Eval. **4**(03), 359–362 (1989)
7. Gerke, K.M., Karsanina, M.V., Katsman, R.: Calculation of tensorial flow properties on pore level: Exploring the influence of boundary conditions on the permeability of three-dimensional stochastic reconstructions. Phys. Rev. E **100**(5), 053312 (2019)
8. Godunov, S.K., Antonov, A.G., Kirilyuk, O.P., Kostin, V.I.: Guaranteed accuracy of solving systems of linear equations in Euclidean spaces. Nauka, Novosibirsk (1992). (in Russian)
9. Khachkova, T., Lisitsa, V., Reshetova, G.: Effect of interface roughness on the elastic properties of 3D layered media. Probab. Eng. Mech. **75**, 103571 (2024)
10. Khachkova, T., Lisitsa, V., Reshetova, G., Tcheverda, V.: Gpu-based algorithm for evaluating the electrical resistivity of digital rocks. Comput. Math. Appl. **82**, 200–211 (2021)
11. Khachkova, T.S., Lisitsa, V.V., Gondul, E.A., Prokhorov, D.I., Kostin, V.I.: Two-phase flow simulation algorithm for numerical estimation of relative phase permeability curves of porous materials. Russ. J. Numer. Anal. Math. Model. **39**(4), 209–221 (2024). https://doi.org/10.1515/rnam-2024-0020
12. Lisitsa, V., Khachkova, T., Sotnikov, O., Islamov, I., Ganiev, D.: Numerical evaluating the permeability of rocks based on correlation dependence on geometry. Lect. Notes Comput. Sci. **14106**, 91–102 (2023). https://doi.org/10.1007/978-3-031-37111-0_7
13. Mostaghimi, P., Blunt, M., Bijeljic, B.: Computations of absolute permeability on micro-CT images. Math. Geosci. **45**(1), 103–125 (2013)
14. Saenger, E.H., et al.: Analysis of high-resolution x-ray computed tomography images of Bentheim sandstone under elevated confining pressures. Geophys. Prospect. **64**(4), 848–859 (2016)
15. Shamsi, A.T., Talabani, S., Vaziri, H., Islam, M.: In-depth investigation of the validity of the archie equation in carbonate rocks. SPE (2001). https://doi.org/10.2118/67204-MS
16. Shulakova, V., et al.: Computational elastic up-scaling of sandstone on the basis of x-ray micro-tomographic images. Geophys. Prospect. **61**(2), 287–301 (2013)
17. Winsauer, W.O., Shearin, H.M. P. H. Masson, Williams, M.: Resistivity of brine-saturated sands in relation to pore geometry. AAPG Bull. **36**(4), 253–277 (1952)
18. Zhan, X., Schwartz, L.M., Toksöz, M.N., Smith, W.C., Morgan, F.D.: Pore-scale modeling of electrical and fluid transport in Berea sandstone. Geophysics **75**(5), F135–F142 (2010)